

Mechanistic modeling of root water uptake in tropical agriculture : a sensitivity analysis of drought stress dynamics

Plant and Soil

de Melo, Marina Luciana Abreu; de Jong van Lier, Quirijn; Heinen, Marius; van Dam, Jos C.; Marin, Fábio Ricardo

https://doi.org/10.1007/s11104-025-07452-0

This publication is made publicly available in the institutional repository of Wageningen University and Research, under the terms of article 25fa of the Dutch Copyright Act, also known as the Amendment Taverne.

Article 25fa states that the author of a short scientific work funded either wholly or partially by Dutch public funds is entitled to make that work publicly available for no consideration following a reasonable period of time after the work was first published, provided that clear reference is made to the source of the first publication of the work.

This publication is distributed using the principles as determined in the Association of Universities in the Netherlands (VSNU) 'Article 25fa implementation' project. According to these principles research outputs of researchers employed by Dutch Universities that comply with the legal requirements of Article 25fa of the Dutch Copyright Act are distributed online and free of cost or other barriers in institutional repositories. Research outputs are distributed six months after their first online publication in the original published version and with proper attribution to the source of the original publication.

You are permitted to download and use the publication for personal purposes. All rights remain with the author(s) and / or copyright owner(s) of this work. Any use of the publication or parts of it other than authorised under article 25fa of the Dutch Copyright act is prohibited. Wageningen University & Research and the author(s) of this publication shall not be held responsible or liable for any damages resulting from your (re)use of this publication.

For questions regarding the public availability of this publication please contact $\frac{openaccess.library@wur.nl}{openaccess.library@wur.nl}$

RESEARCH ARTICLE



Mechanistic modeling of root water uptake in tropical agriculture: a sensitivity analysis of drought stress dynamics

Marina Luciana Abreu de Melo · Quirijn de Jong van Lier · Marius Heinen · Jos C. van Dam · Fábio Ricardo Marin

Received: 2 January 2025 / Accepted: 6 April 2025 © The Author(s), under exclusive licence to Springer Nature Switzerland AG 2025

Abstract

Background and aims Drought stress is a major driver of crop yield reductions in Brazil and other tropical regions. This study explores the mechanistic underpinnings of drought stress using a process-based root water uptake (RWU) model. We aimed to perform a comprehensive sensitivity analysis of the SWAP/MFlux model to simulate drought stress in long-term scenarios of soybean and wheat cultivation under tropical winter-dry conditions.

Methods The agro-hydrological model SWAP, incorporating the RWU function MFlux, was used to simulate 32 years of rainfed soybean and wheat cultivation across five soils with varying hydraulic properties in a tropical winter-dry climate. Sensitivity

Responsible Editor: Hans Lambers.

M. L. A. de Melo (☒) · Q. de Jong van Lier Center for Nuclear Energy in Agriculture, University of São Paulo, P.O. Box 96, Piracicaba, SP, Brazil e-mail: melo.marina@usp.br

M. Heinen

Wageningen Environmental Research, Wageningen, The Netherlands

J. C. van Dam

Soil Physics and Land Management Group, Wageningen University & Research, Wageningen, The Netherlands

F. R. Marin

"Luiz de Queiroz" College of Agriculture (ESALQ), University of São Paulo, Piracicaba, SP, Brazil

Published online: 16 April 2025

analysis of the MFlux function was conducted using three methods — local, global Morris, and global Sobol' — by varying seven RWU parameters within literature-supported ranges.

Results Wheat, grown in the dry winter, experienced higher drought stress than soybean, grown in the wetter summer, across the years. Root length density was the most influential RWU parameter, contributing 35% to 50% of drought stress variation. Soil hydraulic properties were also influential, with Ferralsols linked to a 50% reduction in above-ground dry matter productivity and an Acrisol and a Nitisol to up to 30% in the standard scenario. The Sobol' method provided the most comprehensive parameter sensitivities.

Conclusions Root length density is the most influential parameter in modeling drought stress, with soil hydraulic properties modulating crop responses. This study offers insights for informing management and breeding strategies to mitigate soil- and climate-induced limitations on soybean and wheat production in tropical environments.

Keywords Transpiration · SWAP model · Tropical cultivation · Morris · Sobol'

Introduction

Drought stress, induced by the deficiency of plant available water, is one of the main abiotic factors that limit crop growth, development, and



productivity, affecting food security worldwide (Pandey et al. 2022). This factor is especially relevant to much of the humid tropics, where the El Niño-Southern Oscillation phenomenon has brought reduced rainfall amounts during both the wet and dry seasons (Bunker and Carson 2005; Cai et al. 2020). The scenario has been further aggravated over the last decades by the increase of global surface temperature due to rising greenhouse gas emissions by human activities, mainly related to the use of coal, oil and gases, deforestation, livestock, and farming (Alvares et al. 2022; Marin et al. 2022).

The agriculture sector is particularly affected by climate changes, and within this global issue, Brazil is among the few countries that can still increase agricultural productivity (Anwar et al. 2013; USDA ERS 2022). Over the last two decades, Brazil has emerged as a leading producer of agricultural commodities, including soybeans, grains, cotton, ethanol, and meats. The soybean crop is particularly significant in the expansion of Brazilian agriculture, establishing the country as a top global supplier of commodities (USDA ERS 2022). Nevertheless, the lack of drought-tolerant soybean cultivars in Brazil has been highlighted as a major reason for yield and grain quality losses (Tavares et al. 2022), which poses significant challenges to future expansion in production and trade.

On the other hand, Brazil is one of the largest importers of wheat grains in the world, importing approximately 4.5 million tons annually to complement its internal production (Nóia Júnior et al. 2024). Among the multiple factors compromising wheat production in Brazil, limited soil water availability during growing season ranks as a primary obstacle (Flumignan et al. 2013; Pereira et al. 2019). Hence, developing suitable irrigation practices based on recent studies of crop water use and irrigation management is an urgent demand (Pereira et al. 2023).

The Brazilian agricultural sector faces the challenge of sustaining production growth while adopting sustainable practices, particularly in water use and management (Stevanović et al. 2016). In this context, agro-hydrological models have become indispensable for analyzing soil—water-plant interactions, providing insights into the relationship between water availability and crop performance. These models support the development of strategies to optimize water use and enhance agricultural resilience through improved management practices (Pinto et al. 2023).

A key feature of agro-hydrological models is the simulation of root water uptake (RWU), which is essential for predicting transpiration and crop growth reductions due to drought stress, and provides critical feedback for soil water balance calculations (Jarvis et al. 2022). Process-based RWU models incorporate water potential gradients and hydraulic conductivities or diffusivities to describe water flow within the plant and in the soil toward plant roots (Couvreur et al. 2012; de Jong van Lier et al. 2013, 2008, 2006; de Willigen et al. 2012; Javaux et al. 2013, 2008; Vanderborght et al. 2023, 2021). This process is typically coupled with the dynamic temporal and spatial variations in soil water content via a sink term in the soil water flow equation, facilitating the prediction of soil water potentials with the influence of extracting water by plant roots (Kroes et al. 2017).

In many modeling applications, it is important to assess the sensitivity of model outputs to input factors (variables or parameters). This sensitivity analysis is often necessary, either to deepen understanding of the processes simulated by the model or as an initial step in a model calibration exercise to identify critical system parameters (Doherty 2016). Sensitivity analysis is beneficial as it provides insights into model behavior that are relevant for subsequent model applications. Additionally, it allows for the exclusion of insensitive model parameters from a sequential calibration procedure, thereby reducing computational effort and parameter uncertainty (Stahn et al. 2017).

In a systematic review, Pianosi et al. (2016) distinguished different types of sensitivity analysis (SA). Local SA evaluates how output variability responds to perturbations around specific values of input factors. In contrast, global SA assesses changes across the entire variability space of these factors. Quantitative SA refers to methods where each input factor is associated with a quantitative measure, such as sensitivity indices. Meanwhile, qualitative SA involves visual inspections of model response, often complemented by a subsequent quantitative analysis.

Another qualification proposed by Pianosi et al. (2016) identifies one-at-a-time (OAT) and all-at-a-time (AAT) methods, referring to the sampling strategy used to estimate the sensitivities. In OAT methods, output variations are induced by varying one factor at a time while keeping all others fixed. While local SA typically relies on OAT sampling, OAT can also be applied in global SA by generating sets of



parameter combinations that differ in only one specific parameter value. In contrast, AAT methods for global SA involve varying all input factors simultaneously, considering both the individual influence of each factor and the combined influence due to interactions with other factors. AAT methods usually provide a better assessment of interactions, and some such as variance-based methods, allow the user to evaluate interactions between specific combinations of input factors, such as pairs or triples.

While previous studies have explored parameter sensitivities of RWU models under temperate conditions (Cai et al. 2018; dos Santos et al. 2017), their performance under tropical conditions remains largely unexplored, as differences in rainfall patterns, temperature regimes, and soil water dynamics can lead to distinct soil–water-plant interactions. In this study, the SWAP agro-hydrological model (Kroes et al. 2017), incorporating the recently implemented MFlux transpiration reduction function based on the RWU model of de Jong van Lier et al. (2013, 2008), was used to predict drought stress in soybean and wheat under the conditions of Southeastern Brazil, which features a rainy summer and a dry winter season subject to climate variability.

We present a comprehensive SA of a processbased RWU model using different methods (local and global) and sampling strategies (OAT and AAT), aiming to provide a mechanistic understanding of interactions between tropical climatic conditions, soil hydraulic properties, and plant water uptake.

Material and methods

Climate and soil conditions

Weather data recorded by the weather station of the University of São Paulo in Piracicaba, São Paulo

state, Brazil (22° 42′ 30"S, 47° 38′ 00"W, 546 m a.s.l.) from 1990 to 2021 were used. Historically, the regional climate was classified as subtropical winter-dry with a hot summer (Köppen Cwa). However, in recent decades, climate change has driven a shift toward higher temperatures, and the region is now classified as tropical winter-dry savanna (Köppen Aw) (Alvares et al. 2022). The Aw climate covers approximately 20–30% of Brazilian territory, making it the most common climate in the country, especially in agricultural lands.

The observed annual average rainfall for the period was 1315 mm, and the average minimum ($T_{\rm min}$) and maximum ($T_{\rm max}$) temperatures were 16 °C and 29 °C, respectively. The total rainfall amounts during the meteorological winter and summer seasons (NCEI 2016) are spresented in Table 1.

Five soils under agricultural (arable) use were sampled in São Paulo state. At each location, undisturbed and disturbed soil samples were collected at various depths, following the distribution of the pedological horizons, reaching depths of 60 cm or more. Undisturbed samples were taken using either large rings (approximately 7.4 cm in diameter and 7 cm in height, 10 replicates) or medium rings (approximately 8 cm in diameter and 5 cm in height, 3 replicates). The specific sampling depths for each soil profile corresponded to the center of the layers detailed in Table 6 of Appendix 1. The sampled soils represent three texture classes and three WRB soil orders (Nitisols, Acrisols, and Ferralsols), which are common in the region (Table 2).

The hydraulic properties of the five soils were assessed using undisturbed soil samples in a series of laboratory and field experiments. These included the one-step outflow method using porous plate pressure chambers (applied to all soils), the Hyprop-assisted evaporation method (Peters and Durner 2008) and the falling head saturated permeability laboratory test for the Nitisol

Table 1 Rainfall amounts (mm) observed during the meteorological winter (Jun, Jul, and Aug) and the meteorological summer (Dec, Jan, and Feb) in Piracicaba, São Paulo, Brazil, between 1990 and 2021

	Driest winter	Wettest winter	Driest summer	Wettest summer	
Season (year)	2014	2016	2013/2014	1995/1996	
Rainfall (mm)	38.0	210.6	266.7	873.7	
	Average winter		Average summer		
Rainfall (mm)	103.6 ± 50.6		586.1 ± 151.6		



Table 2 Geographical position, classification, and textural class of the soils sampled in the region of Piracicaba, São Paulo state,

Soil ID	Coordinates	Classification (WRB/FAO) ¹	Textural class
Nitisol	22°42'S, 47°39'W	Eutric Rhodic Ferralic Nitisol	clay
Acrisol	22°42'S, 47°38'W	Eutric Rhodic Acrisol	clay
C. (clayey) Ferralsol	21°15'S, 48°11'W	Eutric Ferralsol	clay
S. L. (sandy loam) Ferralsol	22°21'S, 49°50'W	Dystric Ferralsol	sandy loam
S. (sandy) Ferralsol	22°42'S, 47°37'W	Xanthic Ferralsol	sand

¹World Reference Base (WRB). International soil classification system of the Food and Agriculture Organization of the United Nations (FAO)

and Acrisol, and field internal drainage experiments to determine saturated hydraulic conductivity in the three Ferralsols. Based on measurements of soil water content, pressure head, and soil hydraulic conductivity under saturated and unsaturated conditions, the soil hydraulic properties were expressed as parameters of the van Genuchten (1980) equations with the Mualem (1976) parametric restriction, referred to as VGM hydraulic functions. The obtained VGM parameters for the five sampled soils are presented in Table 6 of Appendix 1.

Modeling seasonal crop growth

The agro-hydrological model SWAP v. 4.2.0, an updated version of the fully documented v. 4.0.1 (Kroes et al. 2017), was used to simulate soybean (*Glycine max*) and wheat (*Triticum* spp.) growing seasons. SWAP was preferred over other models due to its robust handling of soil–water-plant interactions and its proven adaptability to tropical climates (Pinheiro et al. 2019; Pinto et al. 2023). The model inputs included daily meteorological data of solar radiation (kJ m⁻²), minimum and maximum air temperature (°C), water vapor pressure (kPa), wind speed (m s⁻¹), and rainfall (mm) observed in Piracicaba from 1990 to 2021 (32 years), and the soil hydraulic parameters obtained for several layers of the five sampled soils in the region (Appendix 1).

The SWAP model numerically solves a discretized 1D version of the Richards equation with a sink term of root water uptake (Kroes et al. 2017), describing a vertical water flow in the soil as

$$C(h)\frac{\partial h}{\partial t} = \frac{\partial}{\partial z} \left[K(h) \left(\frac{\partial h}{\partial z} + 1 \right) \right] - S(h) \tag{1}$$

where C(h) is the differential water capacity (cm⁻¹), t is time (d), z is the vertical coordinate taken positive upwards (cm), h is the pressure head (cm), K(h) is the soil hydraulic conductivity (cm d⁻¹), and S(h) is the water uptake by plant roots (d⁻¹).

The bottom boundary condition in the simulations was set to free drainage, meaning the downward water flux was driven solely by gravity, with a unit gradient and numerically equal to the hydraulic conductivity of the lowest soil compartment at a depth of 200 cm. The upward upper boundary condition was defined by the simulated evapotranspiration (ET), while the downward upper boundary condition was determined by rainfall minus crop water interception minus runoff.

SWAP firstly calculated potential ET rates (ET_p) using the Penman–Monteith equation (Monteith 1965). ET_p is partitioned between potential plant transpiration (T_p) and potential soil evaporation (E_p) based on the leaf area index or soil cover fraction, which vary according to crop development stage. It also accounts for reductions in T_p and E_p due to soil water fluxes, root water uptake, and crop growth, with reductions occurring from water and/or salt stress. In this study, only drought stress was considered, so the reductions in crop productivity were mainly associated with the rainfall distribution and the soil hydraulic properties.

The detailed crop growth module of SWAP, adapted from the World Food Studies (WOFOST) model (de Wit et al. 2019) was used to simulate crop growth processes. This module enables the simulation of absolute crop productivity (kg ha⁻¹) from conversion factors of assimilates into plant biomass. The potential productivity is calculated as a function of solar radiation, temperature, leaf area, atmospheric



 ${\rm CO}_2$ assimilation, and partitioning factors of produced carbohydrates.

Soybean and wheat cropping cycles were simulated separately and continuously over the years. For soybean, growing seasons were simulated from December 26, 1990, to April 5, 2021, corresponding to 31 seasons (each season starting on Dec 26 and ending on Apr 5 in the subsequent year). Alternatively, wheat growing seasons were simulated from May 30, 1990, to September 22, 2021, corresponding to 32 seasons (starting on May 30 and ending on Sep 22 in the same year). The programmed crop emergence and harvesting dates comprised the rainy season for soybean (the summer) and the dry season for wheat (the winter) (Fig. 1). No irrigation was assumed. During periods without crop growth, the boundary conditions were defined by observed meteorological data, evaporation from bare soil, and free drainage at the bottom of the soil profile.

Crop growth and development parameters were derived from calibrated and validated parameterizations for soybean and wheat from previous studies conducted in Brazil, using the SWAP model with local soil and weather data (de Jong van Lier et al. 2013, 2008; Pinto et al. 2019; Schwantes 2017). Input crop files for this study provide rooting depth as a function of the development stage, with a maximum depth of 60 cm and a uniform distribution over the soil profile. This simplification was adopted to standardize the effect of the root length density parameter in relation to other parameters in the MFlux function,

which do not exhibit depth-related variation. Other key crop parameters used in the simulations are listed in Table 3.

Modeling root water uptake

The simulation of drought stress was conducted using the RWU function MFlux, derived from the process-based RWU model developed by de Jong van Lier et al. (2008, 2013), which describes axisymmetric soil water flow toward individual roots. MFlux applies the matric flux potential (M), a soil hydraulic property defined as the integral of the soil hydraulic conductivity K(h) between a reference pressure head and the target pressure head. The analytical solution for soil water flow, as a function of M, includes parameters such as root radius (r_0) and the radius of the soil cylinder exploited per root, i.e., the rhizosphere radius (r_m) , which may vary with depth according to root length density (L_{RV}) distribution.

Additional parameters describing radial and axial hydraulic resistances within the plant system were introduced by de Jong van Lier et al. (2013), including root tissue hydraulic conductivity (K_{root}), xylem radius (r_x), and hydraulic conductance between leaf and root xylem (K_{stem}). Recently, Heinen et al. (2024) reported the addition of the leaf water potential at which relative transpiration (the ratio of the actual to the potential transpiration) reaches 0.5 ($h_{1/2}$), preventing numerical issues when solving the Richards equation. This parameter, along with the shape parameter

Fig. 1 Average monthly rainfall (mm) and temperature (°C) in Piracicaba between 1990 and 2021 and the simulated growing periods for soybean (26/Dec—5/Apr) and wheat (30/May—22/Sep). Error bars indicate ± the standard deviation

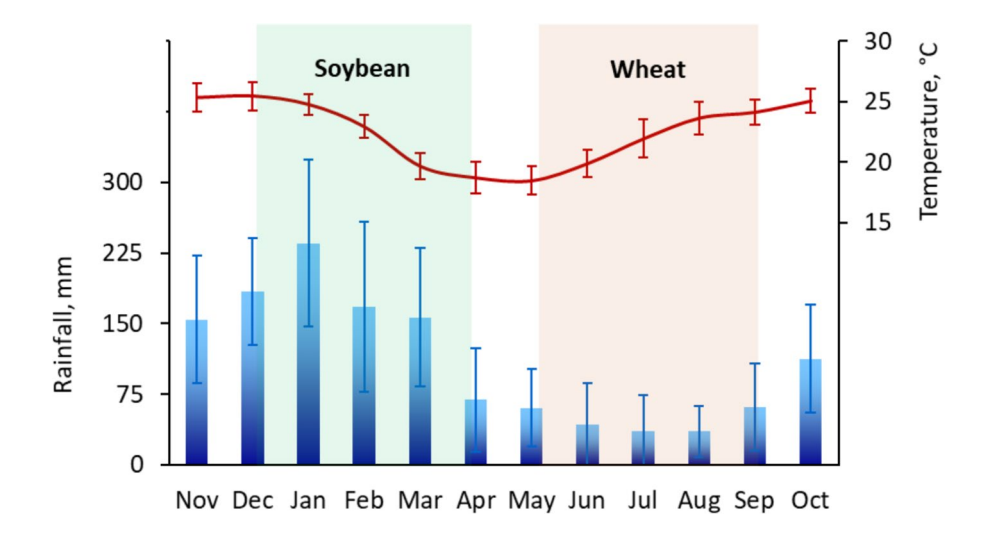




Table 3 Parameters used in the simulations of the soybean and wheat crops in Piracicaba, São Paulo, Brazil

Parameter	Description	Value		
		Soybean	Wheat	
TSUMEA	Temperature sum from emergence to anthesis [°C]	830	1246	
TSUMAM	Temperature sum from anthesis to maturity [°C]	730	1161	
$DTSM_{TAV}$	Increase in temperature sum as function of daily average temperature, <i>TAV</i> [°C]	$0_{\text{TAV}=0-10} \\ 10_{\text{TAV}=20}$	$0_{\text{TAV}=0}$ $30_{\text{TAV}=30}$	
SLA_{DVS}	Specific leaf area as function of development stage, <i>DVS</i> [ha kg ⁻¹]	$25_{\text{TAV}=35-60}$ $1.4 \cdot 10^{-3}_{\text{DVS}=0.00}$ $2.5 \cdot 10^{-3}_{\text{DVS}=0.45}$ $2.5 \cdot 10^{-3}_{\text{DVS}=0.90}$	$30_{\text{TAV}=45}$ $2.2 \cdot 10^{-3}_{\text{DVS}=0.00}$ $2.2 \cdot 10^{-3}_{\text{DVS}=2.00}$	
KDIF	Extinction coefficient for diffuse visible light	$7.0 \cdot 10^{-4}_{\text{DVS}=2.00}$ 0.50	0.60	
KDIF	Extinction coefficient for direct visible light	0.75	0.75	
EFF	Light use efficiency of the leaf [kg ha ⁻¹ h ⁻¹ (J m ⁻² s ⁻¹) ⁻¹]	0.40	0.50	
$AMAX_{DVS0}$	Initial maximum CO ₂ assimilation rate [kg ha ⁻¹ h ⁻¹]	40.0	45.0	
$AMAX_{DVS2}$	Final maximum CO ₂ assimilation rate [kg ha ⁻¹ h ⁻¹]	0.0	45.0	
CVL	Efficiency of conversion into leaves [kg kg ⁻¹]	0.680	0.685	
CVO	Efficiency of conversion into storage organs [kg kg ⁻¹]	0.760	0.779	
CVR	Efficiency of conversion into roots [kg kg ⁻¹]	0.720	0.694	
CVS	Efficiency of conversion into stems [kg kg ⁻¹]	0.690	0.662	
Q10	Relative increase in respiration rate with temperature [$(10 {}^{\circ}\text{C})^{-1}$]	2.00	2.00	

 A_{Camp} , composes the sigmoidal transpiration reduction function of Campbell (1991). The MFlux concept is illustrated in Fig. 2, and the main equations are provided in Appendix 2.

Sensitivity analysis

The effect of the MFlux root water uptake parameters on the simulated drought stress was assessed using the scenarios described in Modeling seasonal crop growth. Drought stress was calculated as the reduction (%) in the simulated above-ground dry matter productivity (kg ha⁻¹) per growing season. An adaptation in the SWAP code was made by setting L_{RV} as an input parameter rather than a variable calculated as a function of the root mass, which is dependent on the crop development stage. Three sensitivity analysis methods were used, which vary in complexity and will be introduced in the following.

• The local method

In the local sensitivity analysis (local SA), the MFlux parameters were varied one-at-the-time, i.e.,

one of the parameters varied while the other parameters remained at baseline values. For each parameter, 40 values were assessed within their respective parameter ranges, defined from a compilation of measured or calibrated values in the literature (Table 4). Exceptions were the parameters r_0 and r_x , which were varied together to avoid physical inconsistency according to $r_x = 0.4 \cdot r_0$ (de Jong van Lier et al. 2013), hereafter referred to as r_0 - r_x . The SEN-SAN program of the PEST suite (Doherty 2016) was linked to the SWAP/MFlux model to automatically perform the model runs and record the simulated drought stress per growing season in each model run.

The local sensitivity (S) was calculated through partial derivatives of the model output function y=f(x), according to

$$S = \frac{\partial y}{\partial x} = \frac{f(x_{i,j}) - f(x_{i,0})}{x_{i,j} - x_{i,0}}$$
(2)

where $x_{i,j}$ is an element of the vector of 40 values for a particular parameter x_i and $x_{i,0}$ is the reference value of x_i .



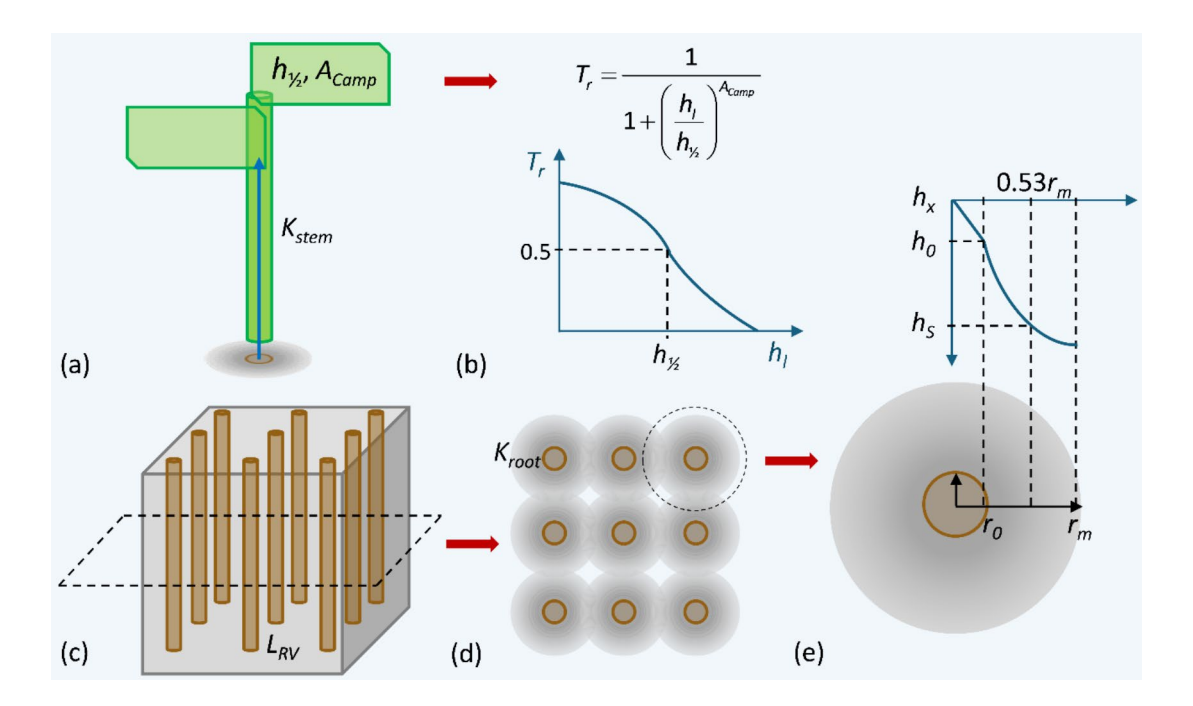


Fig. 2 MFlux concept: a Plant aerial part with the following hydraulic parameters: leaf water potential at which relative transpiration is 0.5 ($h_{1/2}$), exponent in Campbell sigmoidal transpiration reduction function (A_{Camp}), and hydraulic conductance between leaf and root xylem (K_{stem}). b Reduction function of Campbell describing the relationship between leaf water potential (h_1) and relative transpiration (T_r). c Root system as

equally spaced cylinders based on root length density (L_{RV}) . **d** Rhizosphere radius $(r_{\rm m})$, where water moves radially towards the root center at a rate determined by the radial hydraulic conductivity of root tissue (K_{root}) . **e** Radial flow in the rhizosphere, with mean soil pressure head (h_s) corresponding to water potential at $0.53r_{\rm m}$. Schemes based on Vanderborght et al. (2023)

Table 4 Parameterization of the local sensitivity analysis performed with the SWAP/MFlux model

Parameter	Unit	Parameter range ¹	Reference value ¹
Root length density, L_{RV}	cm cm ⁻³	0.01-10.0	2.0
Root radius, r_0	cm	0.005-0.1	0.05
Xylem radius, r_x	cm	0.002-0.04	0.02
Radial hydraulic conductivity of root tissue, K_{root}	$cm d^{-1}$	$4.0 \cdot 10^{-8} - 1.0 \cdot 10^{-5}$	$3.5 \cdot 10^{-6}$
Hydraulic conductance between leaf and root xylem, K_{stem}	d^{-1}	$7.0 \cdot 10^{-5} - 2.1 \cdot 10^{-4}$	$1.0 \cdot 10^{-4}$
Leaf water potential at which relative transpiration is 0.5, $h_{1/2}$	-cm	8000-20000	16600
Exponent in Campbell sigmoidal transpiration reduction function, A_{Camp}	-	5.0-10.0	7.0

¹Sources of parameter ranges and reference values: Campbell (1991), de Jong van Lier et al. (2013, 2008), de Willigen et al. (2012), de Willigen and van Noordwijk (1987), Kremer et al. (2008), Thomas et al. (2024), and Zhuang et al. (2001)

To compare the parameter sensitivities with different dimensions, the average of S over the years was normalized for each parameter as follows:

$$S_{Norm} = \frac{\overline{S}_{x_{i,j}} - \overline{S}_{Min}}{\overline{S}_{Max} - \overline{S}_{Min}}$$
(3)

where $\overline{S}_{x_{i,j}}$ is the average of S over the years for the element $x_{i,j}$ of the vector of values for parameter x_i , and \overline{S}_{Min} and \overline{S}_{Max} are the minimum and maximum average S over the years for parameter x_i , respectively.



Normalization allows for direct comparison of *S* by adjusting for variations in scale caused by differences in parameter magnitudes and units. Without this procedure, larger sensitivities might appear more influential due to scale differences rather than true importance. Rescaling values between 0 and 1 enables fair comparison of the relative contribution of each parameter to system variability.

Equation 3 was applied for each combination of crop (soybean or wheat), soil (Nitisol, Acrisol, C. Ferralsol, S. L. Ferralsol, and S. Ferralsol), and RWU parameter (L_{RV} , r_0 - r_x , K_{root} , K_{stem} , $h_{1/2}$, and A_{Camp}). The average of normalized S and its standard deviation were considered the quantitative outcomes of the local SA.

The Morris method

The Morris method (Morris 1991), also known as the Elementary Effect Test (EET), belongs to the class of one-at-a-time sensitivity analysis designs while allowing the measurement of global sensitivity by aggregating individual sensitivities. In this study, the notation used by Morris (1991) and Saltelli et al. (2008) will be adopted to describe the EET.

A set of input parameters is represented by a vector $x = (x_1, x_2, ..., x_i, ..., x_n)$, where each x_i corresponds to a distinct parameter. Each parameter is normalized to a uniform probability distribution over the interval [0, 1] and is statistically independent of the others. Thus, the domain of x forms a hypercube in parameter space with a side length of 1.0. A p-level grid is then constructed within this hypercube, where each parameter x_i can take discrete values from the set $\{0, 1/(p-1), 2/(p-1), ..., 1\}$. Any parameter x_i assumes values from this discrete set, though not necessarily in adjacent steps. The difference between two discrete values of x_i is denoted as Δ , and this step size is applied to all parameters. For each combination of values of distinct parameters, the model is run to compute an output y. The elementary effect of parameter x_i on the output (EE_i) is calculated from two model runs:

$$EE_{i} = \frac{y(x_{i,1}, x_{i,2}, \dots, x_{i,j-1}, x_{i,j} + \Delta, \dots, x_{i,n}) - y(x_{i,1}, x_{i,2}, \dots, x_{i,n})}{\Delta}$$
(4)

where Δ is a value in $\{1/(p-1), ..., 1-1/(p-1)\}$, in which p is the number of levels of the grid.

Using a random sampling strategy, the model is run multiple times to calculate r values of EE_i . Then, a mean μ and a standard deviation σ are estimated for the probability distribution of EE_i . The statistic μ characterizes the effect of the parameter on the model output, whereas σ characterizes the variability of this influence, a function of model nonlinearity and parameter interactions.

Campolongo et al. (2007) introduced μ^* , the mean of the absolute values of EE_i , providing a more robust representation of nonlinearity and parameter interactions compared to μ , which can diminish due to cancellation in non-monotonic cases (Saltelli et al. 2008). Additionally, for accurate interpretation of parameter ranking, μ^* can be scaled using the standardized EE_i , following Sin and Gernaey (2009):

$$SEE_i = \frac{EEi\sigma(y)}{\sigma(x_i)} \tag{5}$$

where SEE_i is the standardized elementary effect of parameter x_i on the model output y, $\sigma(y)$ is the standard deviation of y and $\sigma(x_i)$ is the standard deviation of parameter x_i . In this study, we used the statistics σ , μ^* , and scaled μ^* .

The Sobol' method

The Sobol' method belongs to the class of variance-based methods for global sensitivity analysis (GSA). It employs the theory proposed by Sobol' (2001), which states that any function of an arbitrary number of parameters can be decomposed into summed functions of parameters taken individually, two by two, three by three, and so on. By discovering and separating these variances, the importance of each parameter to the model output can be revealed, along with the influence of any specific parameter on the model output resulting from its interaction with other parameters (Saltelli et al. 2008, 2004).

Following the theory of Sobol', the total variance V_T of an output y of a model with k input parameters can be decomposed as follows:

$$V_T = V_T(y) = \sum_{i} V_i + \sum_{i} \sum_{j>i} V_{ij} + \dots + V_{12\dots k}$$
 (6)

where:



$$V_{i} = V(E(y|x_{i}))$$

$$V_{ij} = V(E(y|x_{i}, x_{j})) - V_{i} - V_{j}$$
.... (7)

The term $V(E(y|x_i))$ can be interpreted as the variance with respect to parameter x_i of the expected value of y, calculated at multiple values at which x_i is fixed while every other parameter is varied. V_i expresses the so-called first order dependence of y on x_i while V_{ij} expresses the dependence of y on x_i and x_j together; note that the dependence of y on x_i and x_j individually is subtracted from the first term to obtain the collective variance. Similar interpretations apply to higher order terms (White et al. 2020).

The Sobol' method produces two sensitivity indices for each parameter: the first-order sensitivity index (S_i) and the total sensitivity index (S_{Ti}) . The first-order sensitivity index (S_i) is defined as

$$S_i = \frac{V_i}{V_T} \tag{8}$$

where V_i is the first order variance of parameter x_i , and V_T is the total variance of the model output y.

The total sensitivity index (S_{Ti}) includes the sensitivity of y due to first order parameter effects as well as the sensitivity due to interactions between each value assumed by the evaluated parameter and all other parameters. It is defined as

$$S_{Ti} = \frac{E\left[V(y|x_{\sim i})\right]}{V(y)} = 1 - \frac{V\left[E(y|x_{\sim i})\right]}{V(y)}$$
(9)

where $x_{\sim i}$ means all parameters but x_i are allowed to vary, and V(y) is the variance of y.

The Sobol' method requires the number of samples (N) to compute variances. For k parameters, the number of parameter realizations is $N \cdot (k+2)$. To balance the execution of a well-designed variance-based GSA within a reasonable computing time, N typically ranges from a few hundred to a few thousand for k < 20 (Saltelli et al. 2008). In this study, N was set to 400 and k = 6, resulting in 3200 model runs per simulation scenario.

• Applying global methods

To apply the Morris and Sobol' methods to the study scenarios, the program PESTPP-SEN of the Parameter Estimation (PEST) + + suite v. 5.1.23 (White et al.

2020) was linked to the SWAP/MFlux model. Like other programs of PEST ++, PESTPP-SEN obtains case-defining information from a PEST control file. In this file, the upper and lower bounds for parameter variation are specified, along with the observation data. PESTPP-SEN computes parameter sensitivities for each observation/model output pair and for the objective function, defined as

$$\phi = \sum r_i w_i \tag{10}$$

where r_i is the i^{th} residual (the difference between the observation and the respective model output) and w_i is the weight associated with the i^{th} observation.

The upper and lower parameter bounds correspond to those used in the local SA (Table 4). The "observation" data consisted of simulated drought stress per growing season for the standard scenario, defined by the reference parameter values (Table 4), with all values assigned an equal weight of 1. The key PEST + + control variables used to manage the operation of the Morris and Sobol'methods are detailed in Table 5.

Results

Standard scenario

Figure 3 shows simulated drought stress over 32 years of soybean and wheat cultivation in Piracicaba, São Paulo, Brazil, across five soils using the RWU function MFlux with reference parameters. Drought stress patterns were similar for both crops, lowest in the Acrisol and highest in the S. Ferralsol. Year-to-year variability was greater in Ferralsols than in Nitisol and Acrisol (Fig. 3).

Wheat experienced significantly higher drought stress than soybean across all soil types. The 2013/2014 soybean season and the 2014 wheat season recorded the highest stress levels, exceeding 30% and 60%, respectively, due to the driest summer and winter on record (Table 1). In contrast, the 1990 and 2009 wheat seasons showed the lowest stress levels, attributed to more evenly distributed rainfall during these years.

Local parameter sensitivities

From a visual inspection of Fig. 4, the simulated drought stress in soybean appeared relatively



Table 5 PEST + + control variables of the Morris and Sobol' methods for global sensitivity analysis as recommended by Saltelli et al. (2004, 2008)

Variable	Description	Value
Morris method		
$+ + gsa_morris_r()$	Sample size or the number of times that an elementary effect is computed for each parameter x_i (r)	40
$+ + gsa_morris_p()$	Number of levels employed to grid the interval [0, 1] associated with each transformed parameter $x_i(p)$	4
$+ + gsa_morris_delta()$	Parameter variation between two model runs. The default value is $\Delta = p/2[(p-1)]$	0.667
Sobol' method		
$+ + gsa_Sobol_samples()$	Number of samples to use in computing variances, N	400
$+ + gsa_Sobol_par_dis()$	Specifies whether parameter samples are drawn from a uniform or normal distribution. Values are "unif" or "norm"	unif

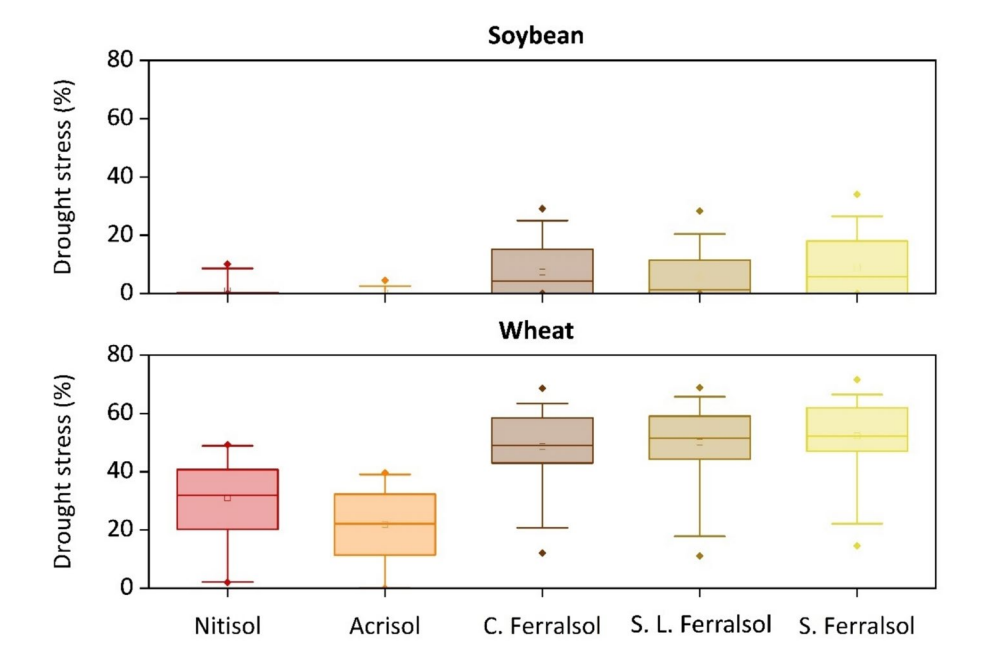


Fig. 3 Drought stress for 32 simulated years of soybean and wheat cultivation in Piracicaba, São Paulo state, Brazil, on five soils (Nitisol, Acrisol, C. Ferralsol, S. L. Ferralsol, and S. Ferralsol). The length of the whiskers is 1.5 times the interquartile range of 25–75%. The parameters of the MFlux function were set at their rseference values: root length density, $L_{RV} = 2.0$ cm

cm⁻³; root radius, r_0 = 0.05 cm; xylem radius, r_x = 0.02 cm; radial hydraulic conductivity of root tissue, K_{root} = $3.5 \cdot 10^{-6}$ cm d⁻¹; hydraulic conductance between leaf and root xylem, K_{stem} = $1.0 \cdot 10^{-4}$ d⁻¹; leaf water potential at which relative transpiration is 0.5, $h_{1/2}$ = 16600 cm; exponent in Campbell sigmoidal transpiration reduction function, A_{Camp} = 7.0

insensitive to K_{stem} and A_{Camp} , moderately sensitive to r_0 - r_x and $h_{1/2}$, and highly sensitive to L_{RV} and K_{root} within the ranges of 0.01—0.10 cm cm⁻³ and 4.0 • 10^{-8} —3.0 • 10^{-8} cm d⁻¹ respectively, across most soil types. For K_{stem} , $h_{1/2}$, and A_{Camp} , the sensitivities often fluctuated between positive and negative values near zero, indicating a non-monotonic relationship.

The soil type affected the simulated drought stress across the parameter ranges, with Ferralsols exhibiting higher drought stress levels (up to 50%) compared to Nitisol and Acrisol. Furthermore, Nitisol and Acrisol showed relatively lower sensitivity to r_0 - r_x than the Ferralsols (Fig. 4).



In the wheat scenarios, higher drought stress values, predominantly exceeding 20%, were simulated across the parameter ranges. Similar to soybean, the highest sensitivities for wheat were observed for L_{RV} followed by K_{root} , particularly at their lowest parameter values. The simulated drought stress for Nitisol and Acrisol showed relatively low sensitivity to r_0 - r_x , K_{stem} , and A_{Camp} , whereas it exhibited slight sensitivity to r_0 - r_x for Ferralsols (Fig. 4).

The local SA method did not account for model nonlinearity or interactions among the RWU parameters. For instance, when assessing the sensitivity of drought stress to K_{root} at three L_{RV} values (0.02, 0.2, and 2.0 cm³ cm⁻³), the local sensitivities increased as L_{RV} decreased, as shown in Fig. 5 for both simulated crops on the sandy loam (S.L.) Ferralsol.

Global parameter sensitivities

Global Morris

The absolute mean (μ^*) and standard deviation (σ) of the elementary effects (EE) of each MFlux parameter on simulated drought stress are shown in Fig. 6. Since the model response was consistent across the three Ferralsols, results are presented only for the Nitisol, the Acrisol, and the S. L. Ferralsol. Parameters with higher μ^* values on the x-axis indicate a greater individual effect, while higher σ values on the y-axis represent a greater degree of interaction with other parameters.

Across all soil and crop scenarios, L_{RV} exhibited the highest μ^* and σ , followed by K_{root} and r_0 - r_x , though at a significant distance. In contrast, the other parameters (K_{stem} , h_{V_2} , A_{Camp}) showed μ^* and σ values close to zero. While r_0 - r_x had a lower individual effect than K_{root} across all scenarios, its degree of interaction was slightly higher in most cases.

Comparing the crops, the μ^* and σ values were lower in the wheat scenarios than in the soybean scenarios, particularly for L_{RV} , K_{root} , and r_0 - r_x . Soil type also influences the degree of parameter sensitivities, with the Nitisol and the Acrisol showing stronger responses compared to the S. L. Ferralsol (Fig. 6).

Global Sobol'

The first-order sensitivity (S_i) and the total sensitivity (S_{Ti}) of each MFlux parameter are shown in Fig. 7

for the Nitisol, the Acrisol, and the S. Ferralsol. The S_i and S_{Ti} values are expressed on the left and the right y-axis, respectively. Across all scenarios, the parameter L_{RV} consistently exhibited the highest S_i and S_{Ti} values, while the sensitivity indices for A_{Camp} remained low.

The second and third highest S_i values were observed for K_{root} and h_{V_2} , respectively, in four soils cultivated with soybean (Nitisol, Acrisol, C. Ferralsol, and S. L. Ferralsol) and two soils cultivated with wheat (Nitisol and Acrisol). For other scenarios, the second and third highest S_i values were obtained for r_0 - r_x and K_{root} , respectively. In contrast, the second-highest S_{Ti} value was observed for K_{root} across all scenarios, with the other parameters exhibiting relatively low S_{Ti} values.

Comparing the crops, S_i values were higher for wheat than for soybean. In the soybean scenarios, S_{Ti} values for each parameter were similar across soils, while in the wheat scenarios, the S_{Ti} value for K_{root} was lower in Ferralsols, as illustrated for the S. Ferralsol (Fig. 7). Despite these crop- and soil-specific differences, the overall model response was consistent across all scenarios regarding Sobol' sensitivities.

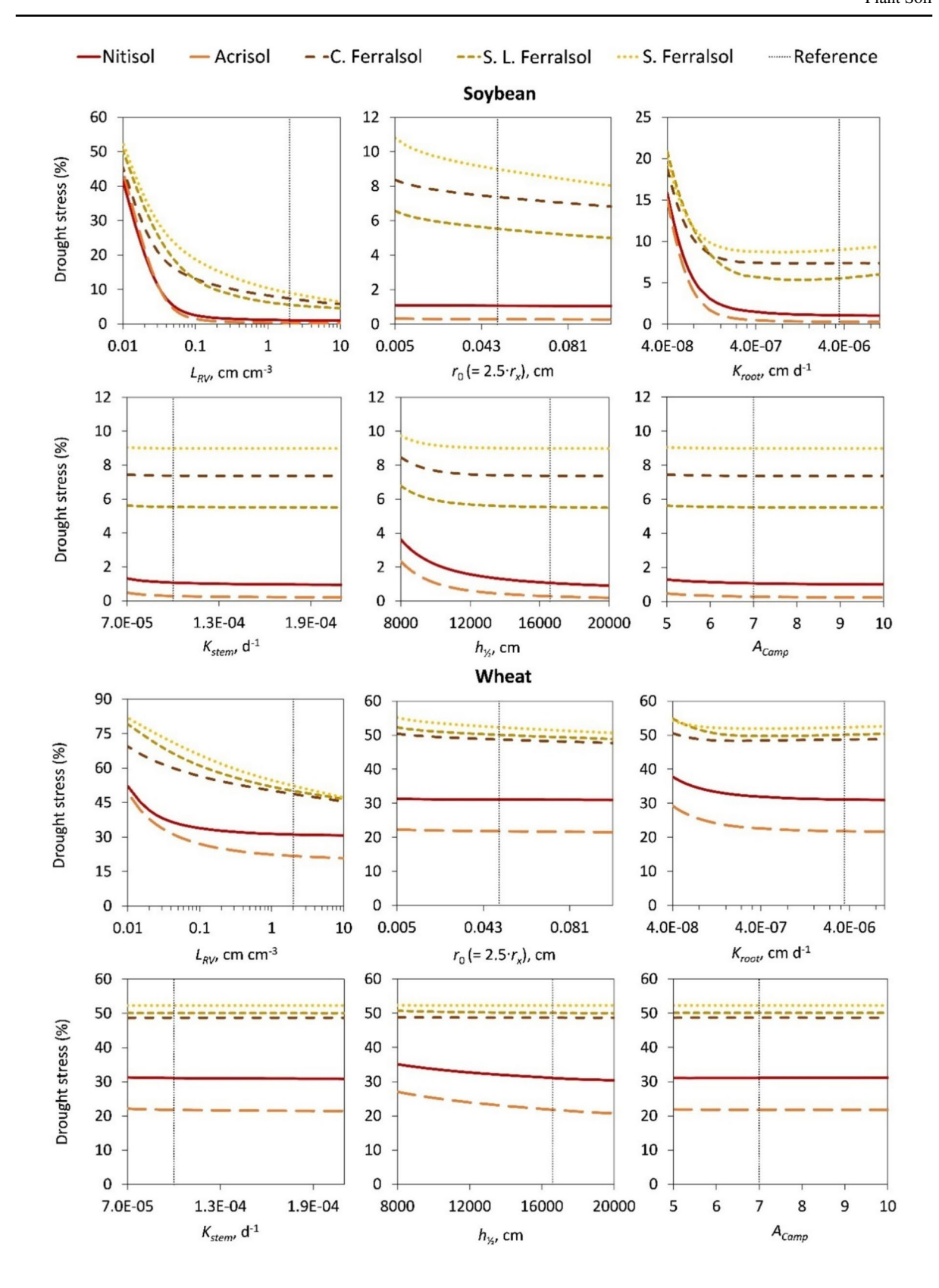
Parameter ranking

Figure 8 shows the ranking of MFlux parameters from each SA method. The local, Morris, and Sobol' sensitivities were calculated using normalized S, scaled μ^* , and average S_i , respectively. For both crops, the local method identified L_{RV} as the most influential parameter, followed by K_{root} . However, the ranking diverged beyond the third position. The composite parameter r_0 - r_x ranked third for wheat but fifth for soybean. The least influential parameter was A_{Camp} for soybean and $h_{1/2}$ for wheat, reflecting their non-monotonic behavior, which resulted in decreased values.

In the Morris method, L_{RV} exhibited the largest contribution to simulated drought stress, while A_{Camp} resulted in the smallest contribution for both crops. The parameter ranking for both crops was similar, with K_{root} ranked second, closely followed by r_0 - r_x , and $h_{1/2}$ and K_{stem} occupying the fourth and fifth positions, respectively.

In the Sobol' method, L_{RV} remained the most influential parameter, while K_{stem} and A_{Camp} showed negligible importance for both crops. For soybean, K_{root}







∢Fig. 4 Drought stress as a function of the MFlux parameters. The results refer to averages of 32 simulated years of soybean and wheat cultivation in Piracicaba, São Paulo, Brazil, on five soils (Nitisol, Acrisol, C. Ferralsol, S. L. Ferralsol, and S. Ferralsol). The dotted vertical line indicates the reference parameter values. L_{RV} is the root length density, r_0 - r_x is the root radius-xylem radius, K_{root} is the radial hydraulic conductivity of root tissue, K_{stem} is the hydraulic conductance between leaf and root xylem, $h_{\frac{1}{2}}$ is the leaf water potential at which relative transpiration is 0.5, and A_{Camp} is the exponent in Campbell sigmoidal transpiration reduction function

and $h_{1/2}$ ranked as the second and third most important parameters, respectively, while for wheat, K_{root} and r_0 - r_x held these positions. The Sobol' method revealed the largest differences between crops, with wheat exhibiting higher sensitivity values. Similarly, the standard deviations of sensitivity indices across soil types were generally larger for wheat than for soybean (Fig. 8).

Discussion

Parameter sensitivities across scenarios

The sensitivity analysis revealed that root length density (L_{RV}) was consistently the most influential parameter in determining simulated drought stress across all simulated scenarios, reaffirming its critical role in modeling root water uptake and its significance for accurately representing soil-plant water interactions (de Jong van Lier et al. 2008, 2013). Lower L_{RV} values correlated with higher drought stress, aligning with experimental and modeling studies showing that denser root systems favor more water extraction (e.g., Couvreur et al. 2012; de Melo et al. 2023; Vanderborght et al. 2021). However, a higher L_{RV} also implies an increased carbon cost for root development, which can influence overall crop yield. While the current model framework does not explicitly account for carbon allocation trade-offs, future model enhancements could integrate this aspect to evaluate how increased root biomass affect aboveground biomass production under varying environmental conditions.

Among the other RWU parameters, radial root conductivity (K_{root}) emerged as the second most

influential parameter, with a notably higher contribution in soils with more favorable hydraulic properties such as the Nitisol and the Acrisol (Fig. 9). This interaction suggests that soil properties modulate the extent to which plant hydraulics influence water uptake. For soils with lower unsaturated hydraulic conductivity, such as the S. Ferralsol (Fig. 9), the sensitivity to parameters like root geometry (r_0 - r_x) became more pronounced (Fig. 7), highlighting the compensatory role of root morphology in mitigating soil limitations to water flow.

Seasonal variability in drought stress simulations reveals the importance of crop-specific dynamics. Wheat, grown in the dry winter season, exhibited higher sensitivity to MFlux parameters than soybean, cultivated during the wetter summer. This result reflects the differential impact of climatic conditions on water stress, with wheat experiencing more challenging water availability conditions compared to soybean. Such findings corroborate previous studies (e.g., Flumignan et al. 2013; Pereira et al. 2023), which emphasize the importance of irrigation management in wheat production, particularly in regions of Brazil where water availability is a limiting factor. This seasonal effect was better captured by Sobol' sensitivities, which offered direct measurements without the need for normalization or scaling when ranking parameters.

Global sensitivity analyses using the Sobol' method provided additional insights into parameter interactions, revealing how soil hydraulic properties and RWU parameters interact dynamically to influence drought stress. While the Nitisol and Acrisol showed a stronger influence of plant hydraulics (e.g., K_{root} and $h_{1/2}$), the Ferralsols exhibited greater dependency on root geometry parameters $(r_0$ - r_x), highlighting the need for tailored model calibration for different soil types. These insights suggest that soil properties can significantly amplify or mitigate the effects of RWU parameters on drought stress predictions, reinforcing the importance of integrating soil and plant hydraulics in agro-hydrological modeling (Vanderborght et al. 2023).

SA methods: merits and shortcomings

The local sensitivity analysis is the simplest method to assess model sensitivities and is often considered poorly



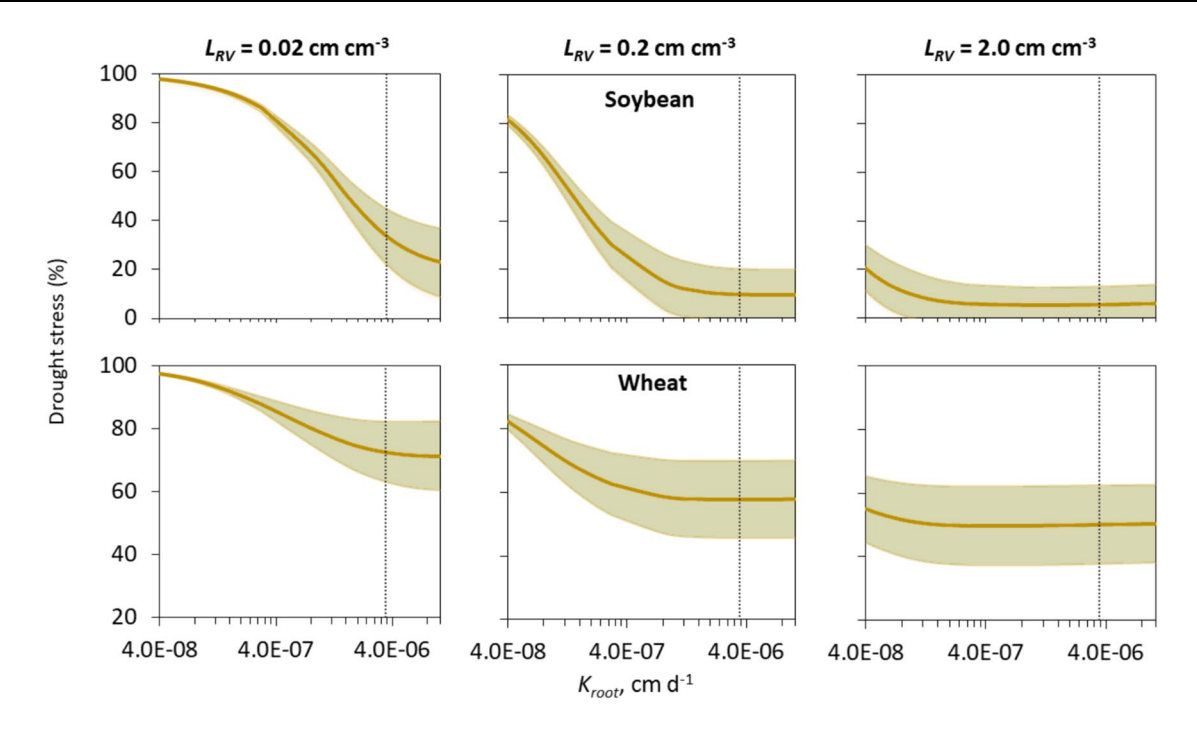


Fig. 5 Drought stress as a function of radial hydraulic conductivity of root tissue (K_{root}) for three values of root length density $(L_{RV} = 0.02, 0.2 \text{ or } 2.0 \text{ cm cm}^{-3})$ applied to simulate soybean and wheat cultivation on the S. L. Ferralsol in Piraci-

caba, São Paulo, Brazil. The shaded area refers to the average \pm the standard deviation for 32 simulated years (1990–2021). The bold line is the average over all years. The dotted vertical line indicates the reference value ($K_{root} = 3.5 \cdot 10^{-6} \, \mathrm{cm \ d^{-1}}$)

efficient. Still, in some cases, it can be informative, e.g., to solve inverse problems or to approximate a model output in the neighborhood of a set of pre-established boundary conditions (Saltelli and Annoni 2010). In our case, we dealt with a nonlinear model incorporating numerous subroutines, including differential equation solvers, demanding a global SA approach to address more complex parameter interactions. Nonetheless, the local partial derivatives proved useful for visualizing and comparing the results from the three SA methods addressed in this study, revealing certain similarities.

The Morris method overcomes the limitation of local sensitivity analysis by calculating partial derivatives at different locations of parameter space. Hence, it can capture parameter interactions, though it is unable to express them apart from model non-linearities (Morris 1991; Saltelli and Annoni 2010). Consequently, a type-I error may occur, i.e., when a parameter is identified as having a significant impact on the model output when, in fact, it does not (Sin and Gernaey 2009). Although the scaled μ^* improves the sensitivity index by standardizing it and reducing

some biases, it cannot eliminate the risk of type-I errors due to inherent limitations of the method, such as sampling constraints and the difficulty of capturing all interactions and nonlinearities.

Among the global sensitivity analysis methods, the Morris method usually requires the fewest sample points. In this study, the computation of the EET statistics (μ^* and σ) required 280 model evaluations, which took approximately 24 h to complete on a conventional laptop computer equipped with an Intel Core i7 -1165G7 processor. Given the high-resolution simulations across multiple scenarios, this runtime is considered relatively small in the context of our research setting. Although practical, the main purpose of this method is to get preliminary and qualitative insights into model sensitivities (Wang and Ierapetritou 2018). Thus, a sequential quantitative method is recommended to avoid potential misinter-pretations (Nguyen and de Kok 2007).

The Sobol' method calculates partial variances, quantifying model sensitivities to multiple parameters through multi-dimensional integrals (Sobol 2001).



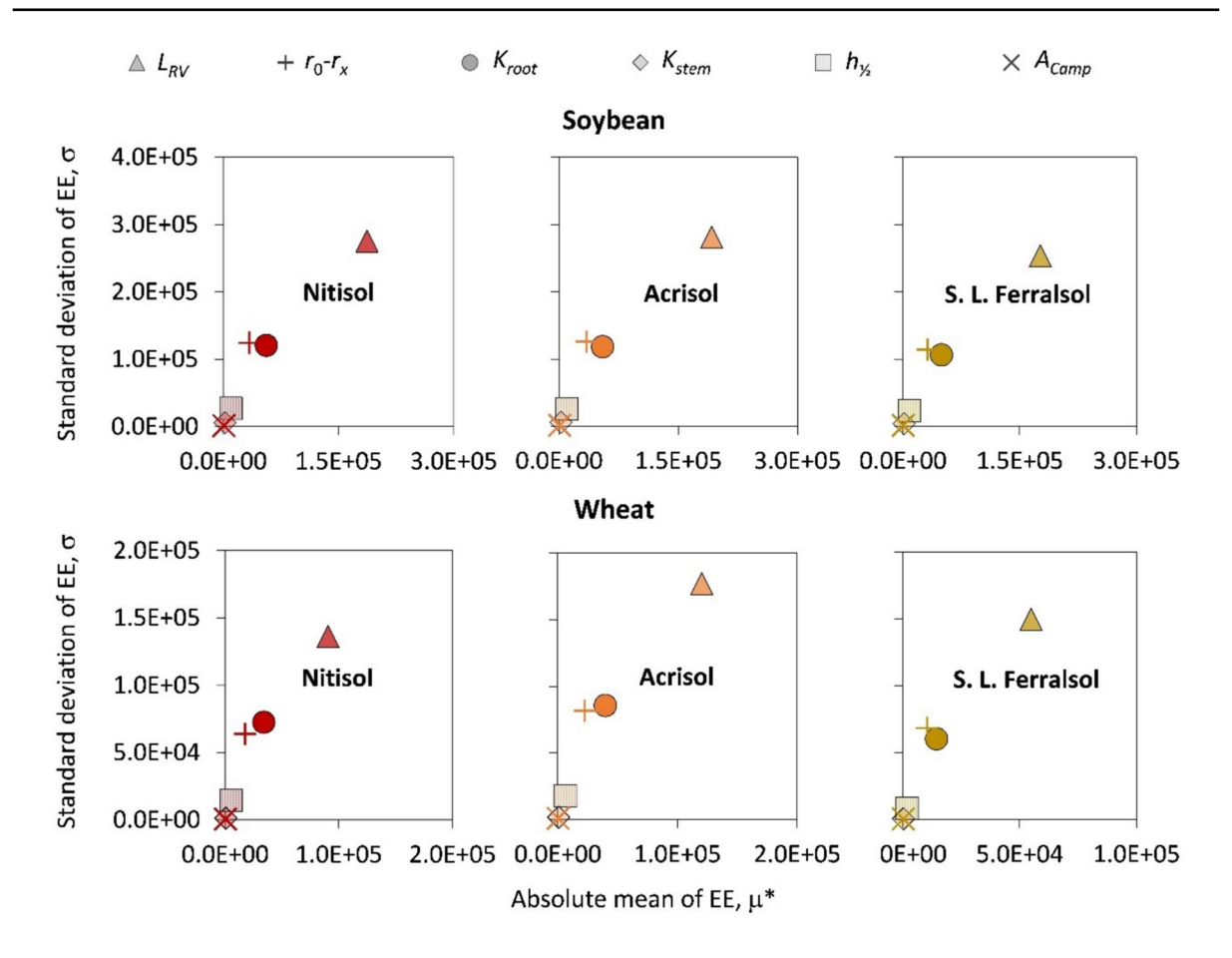


Fig. 6 Absolute mean (μ^*) and standard deviation (σ) of the elementary effects (EE) of the MFlux parameters on simulated drought stress. The results refer to 32 simulated years of soybean and wheat cultivation in Piracicaba, São Paulo, Brazil, on three soils (Nitisol, Acrisol, and S. L. Ferralsol). L_{RV} is the root length density, $r_0 - r_x$ is the root radius-xylem radius, K_{root} is the

radial hydraulic conductivity of root tissue, K_{stem} is the hydraulic conductance between leaf and root xylem, $h_{1/2}$ is the leaf water potential at which relative transpiration is 0.5, and A_{Camp} is the exponent in Campbell sigmoidal transpiration reduction function

The resulting sensitivity indices (S_i and S_{Ti}) are considered powerful and versatile measures, potentially the best practices for performing a sensitivity analysis (Saltelli and Annoni 2010). The Sobol' method effectively handles parameter nonlinearities that cannot be addressed by the other methods used in this study. It can also reveal complex parameter interactions and, by inference, the interaction with the processes to which these parameters pertain (Saltelli et al. 2004; White et al. 2020). Thus, its parameter ranking serves as the most comprehensive guidance for model calibration efforts.

Despite providing a more comprehensive assessment of model sensitivities, the use of the

Sobol' method requires a high number of model evaluations (White et al. 2020), which makes it hardly applicable to computationally demanding models. In this study, the computation of S_i and S_{Ti} required 3200 model runs and took in the order of two weeks on a workstation HP Z230 with Intel® Xenon® E3 v3 processor, which is an unfeasible computer time for many applications of 1D hydrological studies. Hence, this method is computationally unaffordable unless the sensitivity analysis is restricted to only a few model parameters and performed using a relatively fast-running hydrological model on a high-performance computer.



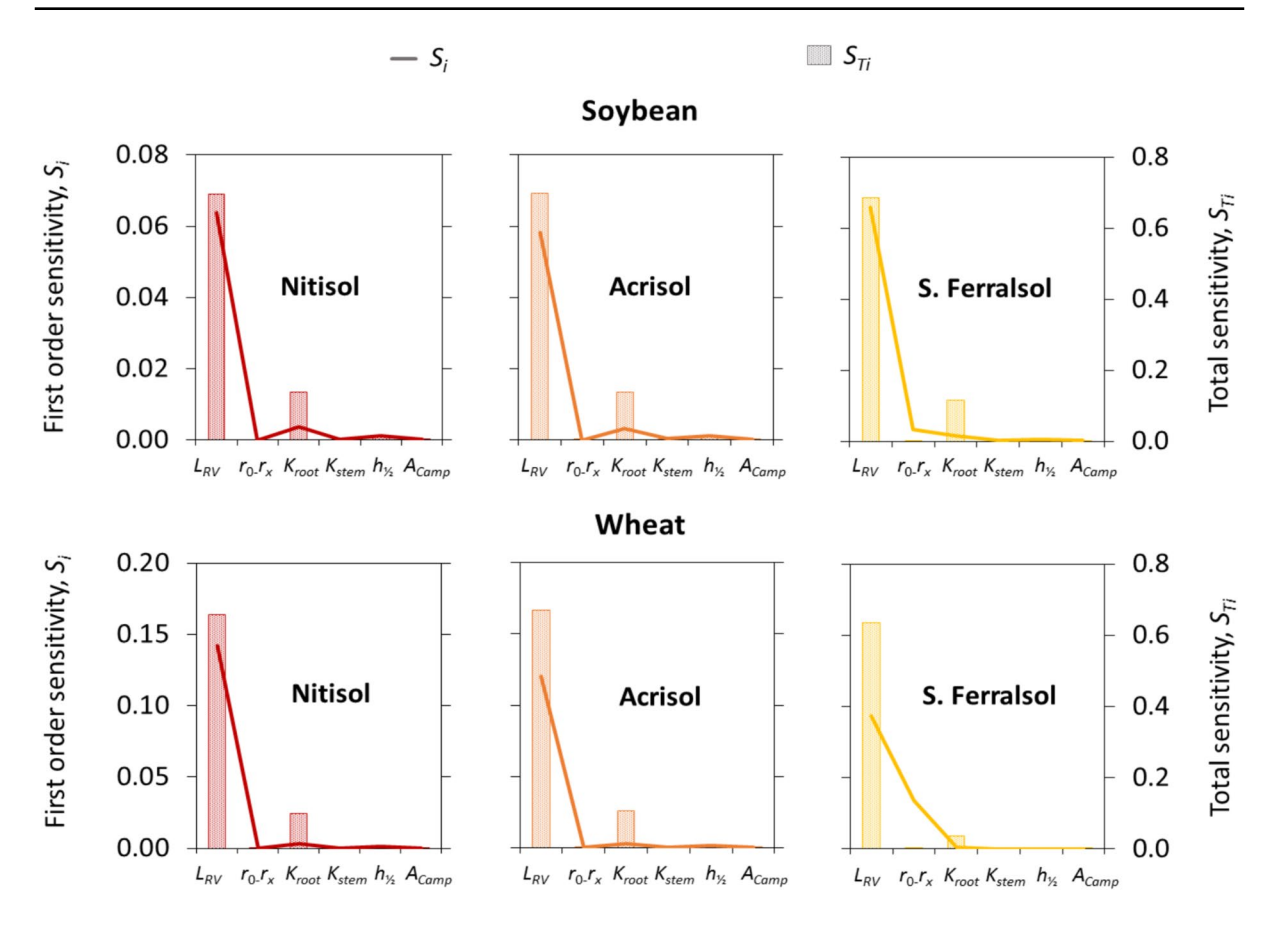


Fig. 7 First order sensitivity (S_i) and total sensitivity (S_{Ti}) of the simulated drought stress to the MFlux parameters. The results refer to the 32 simulated years of soybean and wheat cultivation in Piracicaba, São Paulo, Brazil, on three soils (Nitisol, Acrisol, and S. Ferralsol). L_{RV} is the root length density, r_0 - r_x is the root radius-xylem radius, K_{root} is the radial

hydraulic conductivity of root tissue, K_{stem} is the hydraulic conductance between leaf and root xylem, h_{V_2} is the leaf water potential at which relative transpiration is 0.5, and A_{Camp} is the exponent in Campbell sigmoidal transpiration reduction function

Implications for tropical agriculture

Our findings carry relevant implications for improving agricultural resilience and productivity in tropical regions, particularly under the constraints of climate seasonality and water shortage. By identifying root length density as the most influential parameter in drought stress modeling, this study emphasizes the importance of breeding and management strategies aimed at optimizing root system architecture. An enhanced root system can improve water uptake efficiency (Zhang et al. 2024), mitigating yield losses during periods of low water availability, as observed for both soybean and wheat.

The interactions between soil properties and root water uptake parameters highlight the significance of adapting management practices to specific soil conditions. For instance, the higher drought stress levels simulated for Ferralsols indicates the need for targeted irrigation strategies or soil amendments to enhance water retention. Conversely, in soils with favorable hydraulic properties, such as Nitisols and Acrisols, water management strategies may benefit from a stronger focus on enhancing plant hydraulic parameters, including root conductivity and root xylem conductance.

Seasonal variability in parameter sensitivities further highlights the importance of adapting crop and



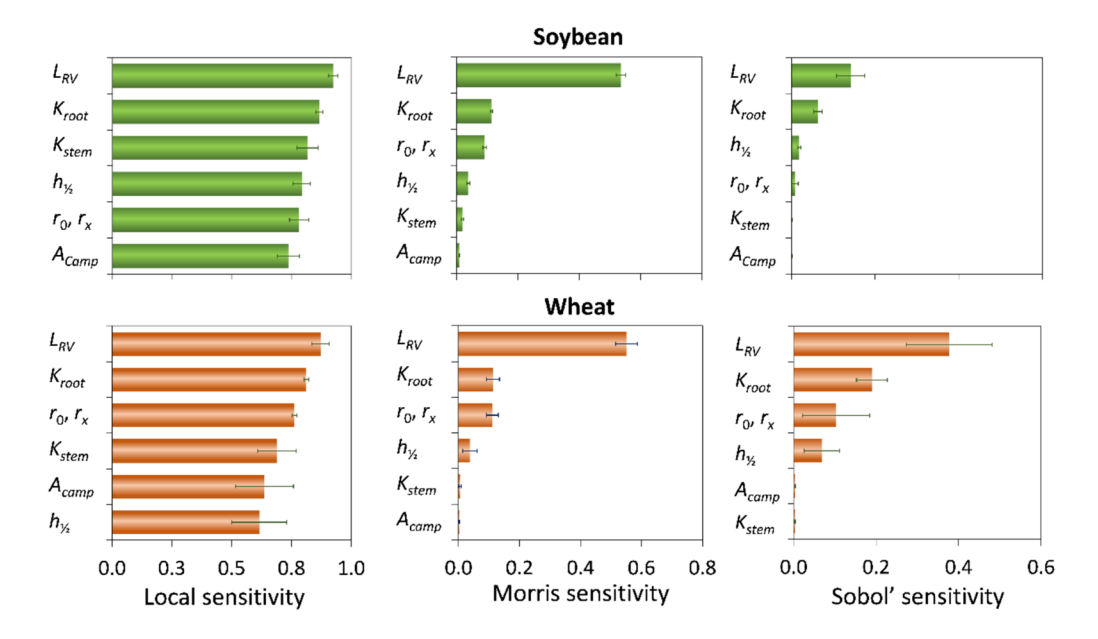


Fig. 8 Parameter ranks of the MFlux parameters according to the local method and two global methods (Morris and Sobol') for sensitivity analysis. The results refer to the average of 32 simulated years of soybean and wheat cultivation in Piracicaba, São Paulo, Brazil, on five soils. Error bars indicate \pm the standard deviation among the evaluated soils. L_{RV} is the root

length density, r_0 - r_x is the root radius-xylem radius, K_{root} is the radial hydraulic conductivity of root tissue, K_{stem} is the hydraulic conductance between leaf and root xylem, h_{y_2} is the leaf water potential at which relative transpiration is 0.5, and A_{Camp} is the exponent in Campbell sigmoidal transpiration reduction function

water management strategies to local climatic conditions. Wheat cultivation, particularly in the dry winter season, showed higher sensitivity to drought stress, indicating that supplemental irrigation systems are critical for stabilizing yields (Nóia Júnior et al. 2024). In contrast, soybean cultivation in the wetter summer season showed resilience under rainfed conditions, if root system traits are adequately optimized (Zhang et al. 2024). These findings align with the increasing emphasis on integrating climate-smart agricultural practices (Bhatnagar et al. 2024) to cope with shifting rainfall patterns and prolonged dry spells in tropical regions.

The SWAP/MFlux model simulates root growth throughout the crop cycle but lacks mechanisms to reduce root growth rates under low soil water availability or adjust maximum rooting depth dynamically. In reality, root depth variations significantly influence water uptake, as plants adapt to soil water content fluctuations. A deeper root system enhances access to subsurface water, mitigating drought stress, especially in low-rainfall seasons (Comas et al. 2013). Root

depth also determines initial soil water storage available for uptake at the start of the cropping cycle. Incorporating dynamic root depth responses to drought stress in future model versions could improve root water uptake predictions in tropical environments.

Direct validation of drought stress predictions could not be performed in this study due to the lack of measurements of above-ground dry matter productivity for the 32 simulated years and under rainfed conditions. Therefore, our findings should be interpreted within the specific context of the simulated conditions. Observations of soil water content, actual crop evapotranspiration, above-ground dry matter productivity, and grain yield from the same location over a three-year period (2016–2018) were analyzed in a separate study, which extends this research, to calibrate the SWAP/MFlux model for soybean and wheat under tropical conditions (de Melo et al. 2025).

Agro-hydrological models like SWAP, enhanced by robust sensitivity analyses, have been valuable tools for guiding agricultural practices (Li and Ren 2019; Lei et al. 2021). The ability to simulate



soil—water-plant interactions under varying climatic, soil, and crop scenarios enables the identification of key factors for improvement, from model parametrization to field-level management strategies (Stahn et al. 2017; Pinheiro et al. 2019). This study also demonstrated the value of advanced techniques, such as Sobol' sensitivity analysis, in uncovering complex parameter interactions and guiding model calibration. These methodological refinements provide a solid foundation for developing strategies to optimize agricultural water use and enhance drought resilience in field crops, ensuring they are oriented by robust, context-specific insights.

Conclusion

Regarding the drought stress predictions of the SWAP/MFlux model, root length density consistently emerged as the most influential parameter across all sensitivity analysis methods, underscoring its critical role in the simulation of transpiration reduction. This finding supports breeding programs and management practices focused on optimizing root system architecture to improve water uptake efficiency.

The interaction between soil hydraulic properties and root water uptake parameters revealed soil-specific dynamics. Drought stress variability across soil types points to the necessity of tailored irrigation and soil amendments to mitigate water limitations and enhance productivity in tropical regions with highweathering soils.

This study offers a comprehensive framework for sensitivity analysis in complex agro-hydrological models, with a focus on root water uptake. By integrating soil, plant, and climate interactions, these models provide valuable tools for sustainable water management in field crops. Our findings support future research aimed at addressing challenges posed by climate variability and soil–water interactions in tropical agriculture.

Author contributions All authors contributed to the study conception and design. Material preparation, data collection and analysis were performed by Marina Luciana Abreu de Melo. Supervision and validation were provided by Quirijn de Jong van Lier, Marius Heinen, Jos C. van Dam, and Fábio

Ricardo Marin. Project administration was performed by Quirijn de Jong van Lier. The first draft of the manuscript was written by Marina Luciana Abreu de Melo and all authors commented on previous versions of the manuscript. All authors have read and approved the final manuscript.

Funding This study was supported by the National Council for Scientific and Technological Development (CNPq, Brazil), grant number 141197/2020–0 and the São Paulo Research Foundation (FAPESP, Brazil), grant numbers 2020/07294–3 and 2022/03770–0.

Data availability The datasets generated during and/or analyzed during the current study are available from the corresponding author on reasonable request.

Declarations

Competing interest The authors declare that they have no known competing financial interests or personal relationships that could influence the opinions reported in this paper.

Appendix 1

The numerical solution of the Richards equation requires parametrization of the unsaturated soil hydraulic properties (K- θ -h). In the SWAP/MFlux model, they are described by the following analytical functions according to Mualem (1976) and van Genuchten (1980):

$$\Theta = \frac{\left(\theta - \theta_r\right)}{\left(\theta_s - \theta_r\right)} = \left[1 + |\alpha h|^n\right]^{(1/n) - 1} \tag{11}$$

$$K = K_s \Theta / \left[1 - \left(1 - \Theta^{n/(n-1)} \right)^{1 - (1/n)} \right]^2$$
 (12)

where Θ is the effective saturation, θ is the soil water content (cm³ cm⁻³), θ_r and θ_s are the residual and saturated soil water content (cm³ cm⁻³), respectively, K_s (cm d⁻¹) is the saturated hydraulic conductivity, and α (cm⁻¹), n, and l are shape parameters.

Eqs. 11 and 12 are the referred VGM hydraulic functions. The soil hydraulic parameters used in the simulations are presented in Table 6. The soil water retention and hydraulic conductivity curves are shown in Fig. 9.



Table 6 Soil hydraulic parameters used in the sensitivity analysis of the SWAP/MFlux model in tropical scenarios

Soil ID	Soil layer (cm)	θ_r (cm ³ cm ⁻³)	θ_s (cm ³ cm ⁻³)	α (cm ⁻¹)	n	l	K_s (cm d ⁻¹)
	0–10	0.237	0.417	0.0290	1.462	0.82	24.6
Nitisol	10-40	0.254	0.402	0.0726	1.157	- 3.45	26.3
	40-200	0.227	0.498	0.1741	1.175	- 4.19	328.2
	0-10	0.142	0.417	0.3431	1.166	1.90	344.4
Acrisol	10-50	0.00	0.481	0.0916	1.087	- 3.97	173.5
	50-200	0.00	0.478	0.1103	1.057	- 5.79	396.7
C. Ferralsol	0-20	0.275	0.463	0.0232	1.389	3.93	76.4
	20-40	0.290	0.447	0.0181	1.356	4.71	113.9
	40-60	0.287	0.444	0.0136	1.443	4.98	120.5
	60-80	0.270	0.506	0.0254	1.591	4.96	1352
	80-200	0.257	0.513	0.0265	1.584	4.97	2014
S. L. Ferralsol	0-15	0.086	0.428	0.0790	1.360	- 0.47	23.3
	15-40	0.123	0.371	0.0394	1.452	8.62	85.9
	40-65	0.152	0.340	0.0171	1.805	6.13	131.5
	65-90	0.133	0.360	0.0168	1.596	- 3.02	152.6
	90-200	0.117	0.340	0.0131	1.482	0.00	102.7
S. Feralsol	0-30	0.293	0.505	0.0172	1.525	8.21	10.4
	30-45	0.272	0.506	0.0169	1.415	8.83	11.1
	45-60	0.289	0.469	0.0219	1.397	5.12	24.0
	60–75	0.289	0.418	0.0095	1.902	3.83	27.3
	75–90	0.255	0.484	0.0201	1.535	0.00	75.1
	90-200	0.271	0.409	0.0092	2.377	0.00	97.4

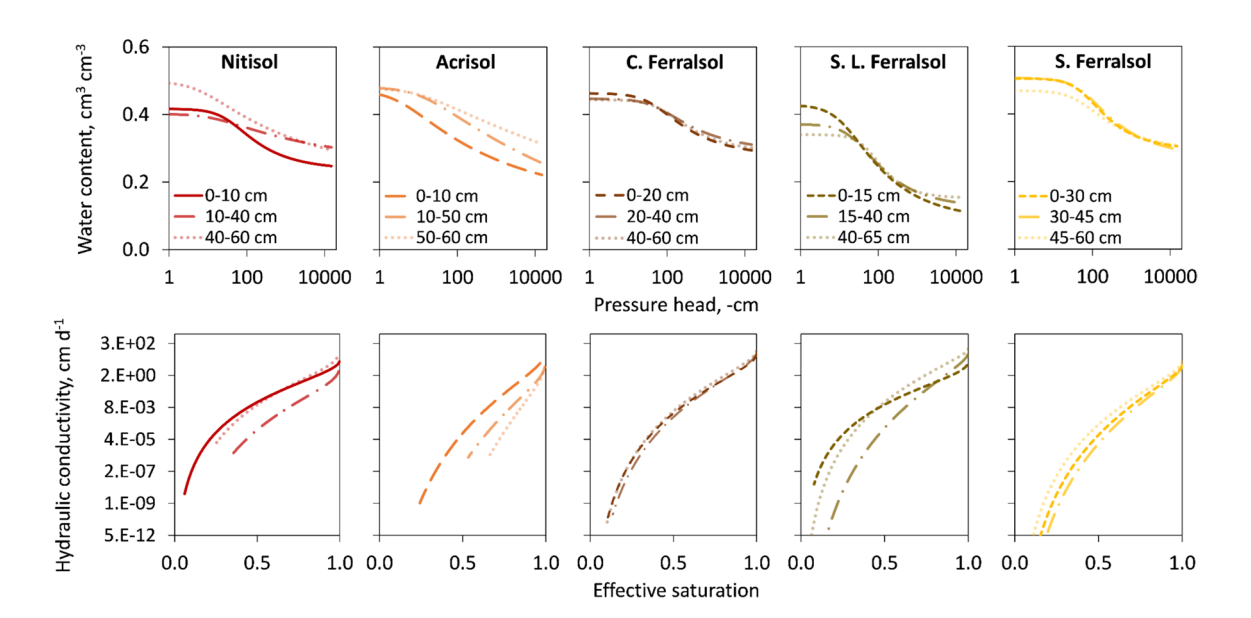


Fig. 9 Soil water retention and hydraulic conductivity curves of the five Brazilian soils used to perform the sensitivity analysis of the SWAP/MFlux model in tropical scenarios. The

X-axes of the water retention curves, and the Y-axes of the hydraulic conductivity curves are on a logarithmic scale



Appendix 2

In the MFlux function, the root system is considered a set of identical cylindrical tubes equally spaced as a function of the root length density, L_{RV} . Under this geometry, a radial flow pattern towards the roots exists and the mass-conservation equation is:

$$\frac{\partial \theta}{\partial t} = -\frac{q}{r} - \frac{\partial q}{\partial r} \tag{13}$$

where θ is the volumetric soil water content (cm³ cm⁻³), t is the time (d), q (cm d⁻¹) is the water flux density, and r (cm) is the radial distance from the root center.

Eq. 13 can be solved defining matric flux potential, M (cm² d⁻¹), a composite soil hydraulic property, as

$$M = \int_{h}^{h} K(h)dh \tag{14}$$

where h_w (cm) is the pressure head at permanent wilting (de Jong van Lier et al. 2013).

The use of *M* allows to write the Darcy equation for soil water flow as

$$q = -K\frac{\partial h}{\partial r} = -\frac{\partial M}{\partial r} \tag{15}$$

For the soil-to-root pathway, de Jong van Lier et al. (2008) developed the following relation between the soil matric flux potential, M_s (cm² d⁻¹) and the RWU rate per unit of volume of a soil layer i, S_i (cm³ cm⁻³ d⁻¹):

$$S_{i} = \frac{4(M_{s,i} - M_{0,i})}{r_{0}^{2} - a^{2}r_{m,i}^{2} + 2(r_{m,i}^{2} + r_{0}^{2})ln\frac{ar_{m,i}}{r_{0}}} = \rho_{i}(M_{s,i} - M_{0,i})$$
(16)

where $M_{0,i}$ (cm² d⁻¹) is the soil matric flux potential at the root surface, r_0 (cm) is the root radius, a is the relative distance between roots at which mean (bulk) soil water content occurs, and $r_{m,i}$ is the rhizosphere radius (cm), which is a function of L_{RV} (cm cm⁻³):

$$r_{m,i} = \sqrt{\frac{1}{\pi L_{RV,i}}} \tag{17}$$

Parameter a was set at the value of 0.53, obtained by de Jong van Lier et al. (2006) for soils described by the VGM hydraulic functions.

The SWAP model also allows to adjust the activity of roots by an empirical factor ranging from 0 to 1 and representing the root system efficiency (R_{eff}):

$$S_i = \rho_i (M_{s,i} - M_{0,i}) R_{eff} \tag{18}$$

Parameter R_{eff} was set at the value of 1 by standard assumption.

To upscale the water uptake from the soil layer to the root system scale, values of S_i for Z soil layers are summed up yielding the total RWU rate, which is equal to the actual transpiration rate, T_a (cm d⁻¹):

$$T_a = \sum_{i=1}^{Z} S_i z_i \tag{19}$$

where z_i is the thickness (cm) of a soil layer i.

The concept of the model was extended by de Jong van Lier et al. (2013) to consider radial and axial plant hydraulic resistances. Within the root, the water content is considered constant, so the hydraulic conductivity does not vary with h:

$$M = \int_{h_{w}}^{h} K(h)dh = K_{root} \int_{h_{w}}^{h} dh = K_{root} (h - h_{w})$$
 (20)

where K_{root} (cm d⁻¹) is the radial hydraulic conductivity of the root tissue.

For the root-to-leaf pathway, the water potential gradient is parameterized by the xylem water potential, h_x (cm) and the leaf water potential, h_l (cm), which are related according to

$$h_x = h_l + \frac{T_a}{K_{stom}} \tag{21}$$

where K_{stem} (d⁻¹) is the hydraulic conductance between leaf and root xylem.

By assuming that the hydraulic properties are constant over the soil-to-root and root xylem-to-leaf pathways, and ignoring any irregularities caused by an imperfect soil-root contact and xylem embolism, the system parameters across the entire pathway (soil-to-root-to-leaf) are expressed by:



$$h_{0,i} + \varphi_i M_{0,i} = h_l + \frac{T_a}{K_{stem}} + \varphi_i M_{s,i}$$
 (22)

where h_0 (cm) is the pressure head at the root surface, and φ_i (d cm⁻¹) is defined by:

$$\varphi_i = \frac{\rho_i r_{m,i}^2 l n_{r_x}^{r_0}}{2K_{root}} \tag{23}$$

where r_x (cm) is the xylem radius.

Eq. 22 contains the unknowns h_0 , h_l , and T_a , whereas M_0 is a function of h_0 . For soils described by the VGM hydraulic functions, no straightforward expression for M(h) exists, but a converging series approximation is available (de Jong Van Lier et al. 2009). Substitution of $M_{0,i}$ in Eq. 18 gives the RWU rate per soil layer, whereas T_a follows from the integration of RWU rates for all soil layers (Eq. 19).

In the updated versions of SWAP (v. 4.2.x), a sigmoidal transpiration reduction function (Campbell 1991; Kremer et al. 2008), referred to as the Campbell function, is incorporated into the MFlux function as

$$T_r = \frac{T_a}{T_p} = \frac{1}{1 + \left(\frac{h_l}{h_{1/2}}\right)^{A_{Camp}}}$$
(24)

where T_r is the relative transpiration, T_p (cm d⁻¹) is the potential transpiration, h_{ν_2} (cm) is the leaf water potential where $T_r = 0.5$, and A_{Camp} is a shape parameter. This equation, in combination with Eq. 22, allows to solve for the values of h_l yielding T_a (Heinen et al. 2024).

References

- Alvares CA, Sentelhas PC, Dias HB (2022) Southeastern Brazil inland tropicalization: Köppen system applied for detecting climate change throughout 100 years of meteorological observed data. Theor Appl Climatol 149:1431– 1450. https://doi.org/10.1007/s00704-022-04122-4
- Anwar MR, Liu DL, Macadam I, Kelly G (2013) Adapting agriculture to climate change: a review. Theor Appl Climatol 113:225–245. https://doi.org/10.1007/s00704-012-0780-1
- Bhatnagar S, Chaudhary R, Sharma S, Janjhua Y, Thakur P, Sharma P, Keprate A (2024) Exploring the dynamics of climate-smart agricultural practices for sustainable

- resilience in a changing climate. Environ Sustain Indic 24:100535. https://doi.org/10.1016/j.indic.2024.100535
- Bunker DE, Carson WP (2005) Drought stress and tropical forest woody seedlings: effect on community structure and composition. J Ecol 93:794–806. https://doi.org/10.1111/j. 1365-2745.2005.01019.x
- Cai G, Vanderborght J, Couvreur V, Mboh CM, Vereecken H (2018) Parameterization of root water uptake models considering dynamic root distributions and water uptake compensation. Vadose Zone J 17:1–21. https://doi.org/10. 2136/vzj2016.12.0125
- Cai W, McPhaden MJ, Grimm AM, Rodrigues RR, Taschetto AS, Garreaud RD, Dewitte B, Poveda G, Ham YG, Santoso A, Ng B, Anderson W, Wang G, Geng T, Jo HS, Marengo JA, Alves LM, Osman M, Li S, Wu L, Karamperidou C, Takahashi K, Vera C (2020) Climate impacts of the El Niño-Southern Oscillation on South America. Nat Rev Earth Environ 1:215–231. https://doi.org/10.1038/s43017-020-0040-3
- Campbell GS (1991) Simulation of water uptake by plant roots.
 In: Hanks J, Ritchie JT (eds) Modeling plant and soil systems. Agronomy Monograph 31. ASA CSSA SSSA, Madison, WI, pp 273–285. https://doi.org/10.2134/agronmonogr31.c12
- Campolongo F, Cariboni J, Saltelli A (2007) An effective screening design for sensitivity analysis of large models. Environ Model Softw 22:1509–1518. https://doi.org/10. 1016/j.envsoft.2006.10.004
- Comas LH, Becker SR, Cruz VMV, Byrne PF, Dierig DA (2013) Root traits contributing to plant productivity under drought. Front Plant Sci 4:442. https://doi.org/10.3389/ fpls.2013.00442
- Couvreur V, Vanderborght J, Javaux M (2012) A simple three-dimensional macroscopic root water uptake model based on the hydraulic architecture approach. Hydrol Earth Syst Sci 16:2957–2972. https://doi.org/10.5194/hess-16-2957-2012
- de Jong van Lier Q, Metselaar K, van Dam JC (2006) Root water extraction and limiting soil hydraulic conditions estimated by numerical simulation. Vadose Zone J 5:1264–1277. https://doi.org/10.2136/vzj2006.0056
- de Jong van Lier Q, van Dam JC, Metselaar K, De Jong R, Duijnisveld W (2008) Macroscopic root water uptake distribution using a matric flux potential approach. Vadose Zone J 7:1065–1078. https://doi.org/10.2136/vzj2007. 0083
- de Jong van Lier Q, van Dam JC, Durigon A, dos Santos MA, Metselaar K (2013) Modeling water potentials and flows in the soil-plant system comparing hydraulic resistances and transpiration reduction functions. Vadose Zone J 12. https://doi.org/10.2136/vzj2013.02.0039
- de Jong van Lier Q, Dourado Neto D, Metselaar K (2009) Modeling of transpiration reduction in van Genuchten– Mualem type soils. Water Resour Res 45. https://doi.org/ 10.1029/2008WR006938
- de Melo MLA, de Jong van Lier Q, Cichota R, Pollacco JAP, Fernández-Gálvez J, Pahlow M (2023) Sensitivity analysis of land and water productivities predicted with an empirical and a process-based root water uptake function. J Hydrol 626:130241. https://doi.org/10.1016/j.jhydrol. 2023.130241



- de Melo MLA, de Jong van Lier Q, da Silva EHFM, Pereira RAA, van Dam JC, Heinen M, Marin FR (2025) Fieldscale modeling of root water uptake and crop growth in a tropical scenario. Field Crops Res 322:109749. https://doi. org/10.1016/j.fcr.2025.109749
- de Willigen P, van Noordwijk M (1987) Roots, plant production and nutrient use efficiency. PhD diss., Wageningen Agric Univ, Wageningen, The Netherlands. https://library.wur.nl/WebQuery/wurpubs/5035. Accessed 12 Dec 2024
- de Willigen P, van Dam JC, Javaux M, Heinen M (2012) Root water uptake as simulated by three soil water flow models. Vadose Zone J 11. https://doi.org/10.2136/vzj2012.0018
- de Wit A, Boogaard H, Fumagalli D, Janssen S, Knapen R, Van Kraalingen D, Supit I, Van Der Wijngaart R, Van Diepen K (2019) 25 years of the WOFOST cropping systems model. Agric Syst 168:154–167. https://doi.org/10.1016/j. agsy.2018.06.018
- Doherty J (2016) PEST model-independent parameter estimation user manual part I: PEST, SENSAN and global optimisers. Watermark Numerical Computing 6. https://www.epa.gov/sites/default/files/documents/PESTMAN.PDF. Accessed 1 Feb 2024
- dos Santos MA, de Jong van Lier Q, van Dam JC, Freire Bezerra AH (2017) Benchmarking test of empirical root water uptake models. Hydrol Earth Syst Sci 21:473–483. https://doi.org/10.5194/hess-21-473-2017
- Flumignan DL, Lena BP, Faria RT, Scholz MBS, Medina CC (2013) Influence of irrigation on wheat crop. Eng Agric 33:75–88. https://doi.org/10.1590/S0100-6916201300 01000009
- Heinen M, Mulder M, van Dam J, Bartholomeus R, de Jong van Lier Q, de Wit J, de Wit A, Hack-ten Broeke M (2024) SWAP 50 years: advances in modeling soil-water-atmosphere-plant interactions. Agric Water Manag 298:108883. https://doi.org/10.1016/j.agwat.2024.108883
- Jarvis N, Larsbo M, Lewan E, Garré S (2022) Improved descriptions of soil hydrology in crop models: the elephant in the room? Agric Syst 202:103477. https://doi. org/10.1016/j.agsy.2022.103477
- Javaux M, Schröder T, Vanderborght J, Vereecken H (2008) Use of a three-dimensional detailed modeling approach for predicting root water uptake. Vadose Zone J 7:1079– 1088. https://doi.org/10.2136/vzj2007.0115
- Javaux M, Couvreur V, Vanderborght J, Vereecken H (2013) Root water uptake: from three-dimensional biophysical processes to macroscopic modeling approaches. Vadose Zone J 12. https://doi.org/10.2136/vzj2013.02.0042
- Kremer C, Stöckle CO, Kemanian AR, Howell T (2008) A canopy transpiration and photosynthesis model for evaluating simple crop productivity models. Adv Agric Syst Model 1:165–189. https://doi.org/10.2134/advagricsystmodel1. c6
- Kroes JG, van Dam JC, Bartholomeus RP, Groenendijk P, Heinen M, Hendriks RFA, Mulder HM, Supit I, van Walsum PEV (2017) SWAP version 4. https://doi.org/10. 18174/416321
- Lei G, Zeng W, Jiang Y, Ao C, Wu J, Huang J (2021) Sensitivity analysis of the SWAP (Soil-Water-Atmosphere-Plant) model under different nitrogen applications and root distributions in saline soils. Pedosphere 31:807–821. https://doi.org/10.1016/S1002-0160(21)60038-3

- Li P, Ren L (2019) Evaluating the effects of limited irrigation on crop water productivity and reducing deep groundwater exploitation in the North China Plain using an agrohydrological model: I. Parameter sensitivity analysis, calibration and model validation. J Hydrol 574:497–516. https://doi.org/10.1016/j.jhydrol.2019.04.053
- Marin FR, Zanon AJ, Monzon JP, Andrade JF, Silva EH, Richter GL, Antolin LAS, Ribeiro BSMR, Ribas GG, Battisti R, Heinemann AB, Grassini P (2022) Protecting the Amazon forest and reducing global warming via agricultural intensification. Nat Sustain 5:1018–1026. https://doi.org/10.1038/s41893-022-00968-8
- Monteith JL (1965) Evaporation and environment. Symp Soc Exp Biol 19:205–234
- Morris MD (1991) Factorial sampling plans for preliminary computational experiments. Technometrics 33:161–174. https://doi.org/10.2307/1269043
- Mualem Y (1976) A new model for predicting the hydraulic conductivity of unsaturated porous media. Water Resour Res 12:513–524. https://doi.org/10.1029/WR012i003p00513
- NCEI (2016) Meteorological versus astronomical seasons. National Centers for Environmental Information (NCEI). https://www.ncei.noaa.gov/news/meteorological-versus-astronomical-seasons. Accessed 1 Apr 2024
- Nguyen TG, de Kok JL (2007) Systematic testing of an integrated systems model for coastal zone management using sensitivity and uncertainty analyses. Environ Model Softw 22:1572–1587. https://doi.org/10.1016/j.envsoft.2006.08.008
- Nóia Júnior RS, Nardino M, Elli EF, Pequeno D, Fraisse C, Asseng S (2024) Achieving wheat self-sufficiency in Brazil. Environ Res Lett 19:031003. https://doi.org/10. 1088/1748-9326/ad26b8
- Pandey VC, Gajić G, Sharma P, Roy M (2022) Soil and phytomanagement for adaptive phytoremediation practices. In: Pandey VC, Gajić G, Sharma P, Roy M (eds) Adaptive phytoremediation practices. Elsevier, pp 135–179. https://doi.org/10.1016/B978-0-12-823831-8.00002-5
- Pereira JF, Cunha GR, Moresco ER (2019) Improved drought tolerance in wheat is required to unlock the production potential of the Brazilian Cerrado. Crop Breed Appl Biotechnol 19:217–225. https://doi.org/10.1590/1984-70332019v19n2r30
- Pereira RAA, Silva EHFM, Gonçalves AO, Vianna MS, Silva TJA, Fenner W, Vieira PVD, Marin FR (2023) Winter wheat evapotranspiration and irrigation requirements across tropical and sub-tropical producing regions in Brazil. Theor Appl Climatol 151:375–388. https://doi.org/10.1007/s00704-022-04282-3
- Peters A, Durner W (2008) Simplified evaporation method for determining soil hydraulic properties. J Hydrol 356:147–162. https://doi.org/10.1016/j.jhydrol.2008.04. 016
- Pianosi F, Beven K, Freer J, Hall JW, Rougier J, Stephenson DB, Wagener T (2016) Sensitivity analysis of environmental models: a systematic review with practical workflow. Environ Model Softw 79:214–232. https://doi.org/10.1016/j.envsoft.2016.02.008
- Pinheiro EAR, van Lier QDJ, Šimůnek J (2019) The role of soil hydraulic properties in crop water use efficiency: a process-based analysis for some Brazilian scenarios.



- Agric Syst 173:364–377. https://doi.org/10.1016/j.agsy. 2019.03.019
- Pinto VM, van Dam JC, de Jong van Lier Q, Reichardt K (2019) Intercropping simulation using the SWAP model: development of a 2×1D algorithm. Agric 9:126. https://doi.org/10.3390/agriculture9060126
- Pinto VM, de Borja Reis AF, de Melo MLA, Reichardt K, Santos D, de Jong van Lier Q (2023) Sustainable irrigation management in tropical lowland rice in Brazil. Agric Water Manag 284:108345. https://doi.org/10.1016/j. agwat.2023.108345
- Saltelli A, Annoni P (2010) How to avoid a perfunctory sensitivity analysis. Environ Model Softw 25:1508–1517. https://doi.org/10.1016/j.envsoft.2010.04.012
- Saltelli A, Tarantola S, Campolongo F, Ratto M (2004) Sensitivity analysis in practice: a guide to assessing scientific models. Wiley Online Library. https://doi.org/10.1002/0470870958
- Saltelli A, Ratto M, Andres T, Campolongo F, Cariboni J, Gatelli D, Saisana M, Tarantola S (2008) Global sensitivity analysis. Wiley, The primer. https://doi.org/10.1002/ 9780470725184
- Schwantes AP (2017) Agricultural resource efficiency and reduction of impacts under land-use and climate change scenarios in Brazil. PhD diss., University of São Paulo, Piracicaba, Brazil. https://doi.org/10.11606/T.11.2017.tde-02102017-094321
- Sin G, Gernaey KV (2009) Improving the Morris method for sensitivity analysis by scaling the elementary effects. In: Jeżowski J, Thullie J (eds) Computer aided chemical engineering. Elsevier, pp 925–930. https://doi.org/10.1016/ S1570-7946(09)70154-3
- Sobol' IM (2001) Global sensitivity indices for nonlinear mathematical models and their Monte Carlo estimates. Math Comput Simul 55:271–280. https://doi.org/10.1016/ S0378-4754(00)00270-6
- Stahn P, Busch S, Salzmann T, Eichler-Löbermann B, Miegel K (2017) Combining global sensitivity analysis and multiobjective optimisation to estimate soil hydraulic properties and representations of various sole and mixed crops for the agro-hydrological SWAP model. Environ Earth Sci 76:367. https://doi.org/10.1007/s12665-017-6701-y
- Stevanović M, Popp A, Lotze-Campen H, Dietrich JP, Müller C, Bonsch M, Schmitz C, Bodirsky BL, Humpenöder F, Weindl I (2016) The impact of high-end climate change on agricultural welfare. Sci Adv 2:e1501452. https://doi.org/10.1126/sciadv.1501452
- Tavares CJ, Ribeiro Junior WQ, Ramos MLG, Pereira LF, Casari RACN, Pereira AF, de Sousa CAF, da Silva AR, Neto SPS, Mertz-Henning LM (2022) Water stress alters morphophysiological, grain quality and vegetation indices of soybean cultivars. Plants 11:559. https://doi.org/10. 3390/plants11040559
- Thomas A, Yadav BK, Šimůnek J (2024) Water uptake by plants under nonuniform soil moisture conditions: a

- comprehensive numerical and experimental analysis. Agric Water Manag 292:108668. https://doi.org/10.1016/j.agwat.2024.108668
- USDA ERS (2022) Brazil's momentum as a global agricultural supplier faces headwinds. https://www.ers.usda.gov/amber-waves/2022/september/brazil-s-momentum-as-aglobal-agricultural-supplier-faces-headwinds. Accessed 27 Dec 2023
- van Genuchten MT (1980) A closed-form equation for predicting the hydraulic conductivity of unsaturated soils. Soil Sci Soc Am J 44:892–898. https://doi.org/10.2136/sssaj 1980.03615995004400050002x
- Vanderborght J, Couvreur V, Meunier F, Schnepf A, Vereecken H, Bouda M, Javaux M (2021) From hydraulic root architecture models to macroscopic representations of root hydraulics in soil water flow and land surface models. Hydrol Earth Syst Sci 25:4835–4860. https://doi.org/10.5194/hess-25-4835-2021
- Vanderborght J, Leitner D, Schnepf A, Couvreur V, Vereecken H, Javaux M (2023) Combining root and soil hydraulics in macroscopic representations of root water uptake. Vadose Zone J n/a, e20273. https://doi.org/10.1002/vzj2.20273
- Wang Z, Ierapetritou M (2018). Chapter 8 Global sensitivity, feasibility, and flexibility analysis of continuous pharmaceutical manufacturing processes, in: Singh, R., Yuan, Z. (Eds.), Computer Aided Chemical Engineering, Process Systems Engineering for Pharmaceutical Manufacturing. Elsevier, pp. 189–213. https://doi.org/10.1016/B978-0-444-63963-9.00008-7
- White, JT, Hunt, RJ, Fienen, MN, Doherty, JE (2020). Approaches to highly parameterized inversion: PEST++ Version 5, a software suite for parameter estimation, uncertainty analysis, management optimization and sensitivity analysis (No. 7-C26), Techniques and Methods. U.S. Geological Survey. https://doi.org/10.3133/tm7C26
- Zhang Y, Wu X, Wang X, Dai M, Peng Y (2024) Crop root system architecture in drought response. J Genet Genom. https://doi.org/10.1016/j.jgg.2024.05.001
- Zhuang J, Nakayama K, Yu G-R, Urushisaki T (2001) Estimation of root water uptake of maize: an ecophysiological perspective. Field Crops Res 69:201–213. https://doi.org/10.1016/S0378-4290(00)00142-8

Publisher's Note Springer Nature remains neutral with regard to jurisdictional claims in published maps and institutional affiliations.

Springer Nature or its licensor (e.g. a society or other partner) holds exclusive rights to this article under a publishing agreement with the author(s) or other rightsholder(s); author self-archiving of the accepted manuscript version of this article is solely governed by the terms of such publishing agreement and applicable law.

